

1 **Hydrological study and assessment of water budget for Erbil basin,**
2 **Kurdistan region, Iraq**

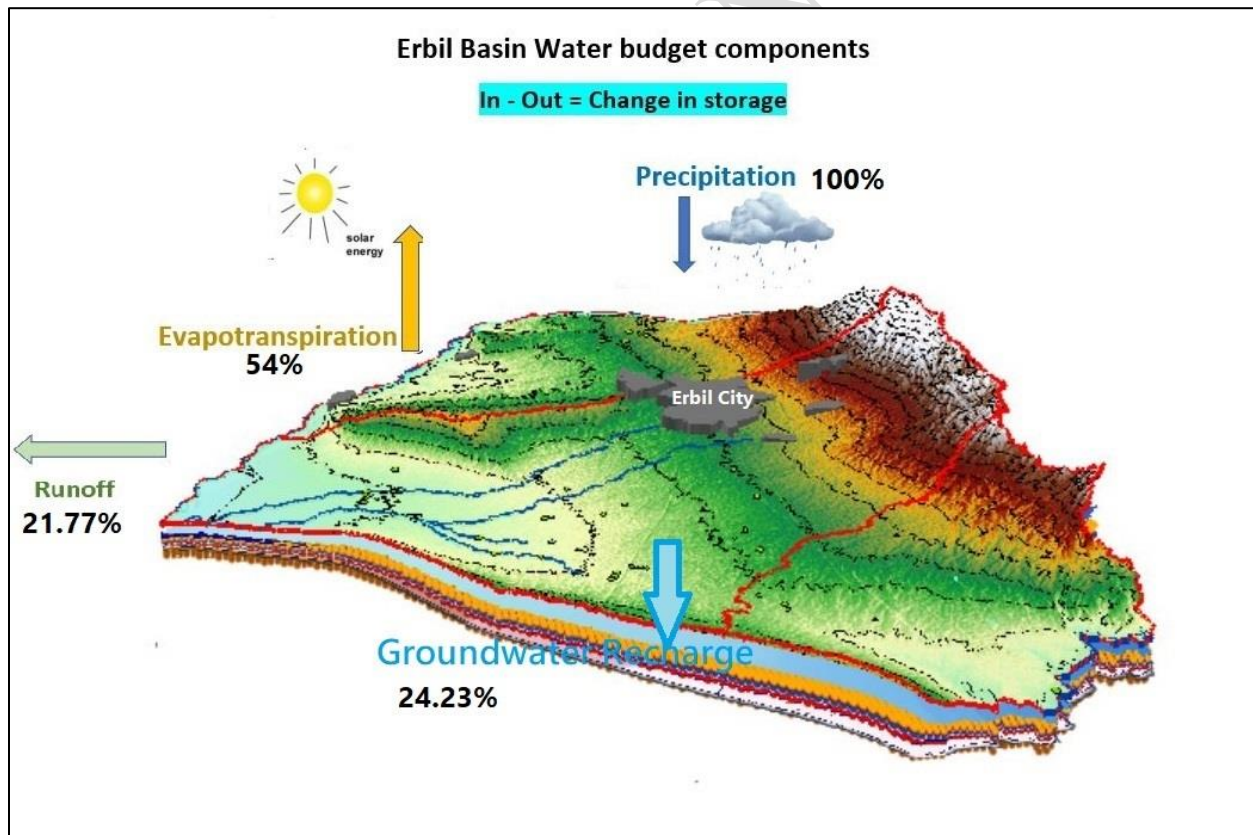
3
4 **Jwan Sabah Mustafa^{1*}, Dana Khider Mawlood^{1,2}**

5 ¹Department of Civil Engineering, College of Engineering, Salahaddin University, Erbil, Iraq.

6 ² Vice president in University of Kurdistan-Hawler (UKH), Erbil, Iraq.

7 *Corresponding author: E-mail: (juan.sabah@yahoo.com or jwan.mustafal@su.edu.krd), tel:
8 (096407503519599)

9
10 **GRAPHICAL ABSTRACT**



11
12
13 **ABSTRACT**

14 This research is conducted on Erbil basin, it is located in northern part of Iraq, the basin is composed
15 of three main sub-basins which are: Northern part (Kapran), Central sub-basin and Southern part
16 (Bashtepa) respectively. The total area of three sub-basins is approximately (3,200 km²). The main
17 sources of aquifer recharge in the study area is depends on precipitation. The article estimated the
18 percentage and amount of water budget elements for the selected basin. Therefore, the paper
19 evaluates the obtained climate data form Erbil meteorological station for (25 years) to evaluate the
20 water budget in the study area. The main objective to assess the Erbil basin water budget and
21 determine amount of the each parameters related to the study area. Based on the results of this study
22 data analysis the amount of the mean monthly temperature (18.94 °C), and sun shine (8.18 hr/day),
23 the average relative humidity is (47.82%), the evaporation percentage is (54%) of the precipitation.
24 The study concluded that the amonut of the rainfall data is (394.65mm) and the percentage of
25 precipitation over Erbil basin is (100%), the Recharge into groundwater is (24.23%), the Runoff and
26 Evporation are (21.77%) and (54%) respectively. The study employed the MODFLOW-2000
27 package within the Groundwater Modeling System (GMS), a computer program utilizing a finite
28 difference numerical method to solve three-dimensional groundwater flow equations. Conducted on
29 the Erbil plain, the research aimed to develop an acceptable and calibrated model, shedding light on
30 the hydraulic properties of the aquifer systems in the region. Calibration was achieved by comparing
31 observed field values with simulated heads, resulting in a good coefficient of determination. The
32 findings highlight the significance of groundwater modeling as a powerful tool for managing and
33 planning aquifer systems in any selected region. By providing a detailed understanding of the
34 groundwater dynamics in the Erbil basin, this study contributes to the sustainable use of water
35 resources and facilitates informed decision-making for future development and conservation efforts.
36 The research underscores the broader applicability of groundwater modeling in addressing water
37 management challenges and emphasizes its role in supporting environmentally sound practices for
38 the benefit of communities and ecosystems.

39 **Keywords:** Hydrological study, Evaporation, Recharge, Runoff, Rainfall, Water balance, GMS.

ACCEPTED MANUSCRIPT

40 **1. Introduction**

41 The study area was characterized as being located in an arid or semi-arid region, therefore, it
42 was deemed essential that water demand in the region be provided by management. The area was
43 determined to have high values of the evaporation rate and water recharge to the ground. Meanwhile,
44 the area was also characterized as having high velocity with low duration that could lead to flooding
45 (Fathy et al., 2021). The study area was mainly depended on by rainfall to recharge the aquifers in
46 the area. Since, water demand was increased with the increasing population growth. The climate and
47 hydrogeological condition of any area were reflected by the nature of the area which directly
48 impacted the hydrological cycle. The principle of the water balance equation was applied as the
49 application of the mass conservation law, and was mainly referred to as the continuity equation.
50 That, said the difference between all the input and output for any control volume and period were
51 balanced by the change in storage. In this study, the water balance application was used to predict
52 the consequences of artificial changes in the groundwater basins (Al sudani, 2019). Erbil basin was
53 divided into three main sub-basins that were: (Kapran, Central, and Bashtepa) also called as
54 (Northern, central and Southern) respectively. The rock of the study area consisted of the (Upper
55 Miocene – Recent) and which was mainly consisted; Muqdadiya, Bai Hassan formations and also
56 Quaternary deposits (Hassan, 1998). While, several previous studies had calculated water balance
57 for particular locations, from these studies that were conducted in Erbil area are; the
58 Hydrogeological Study of Central sub-basin (Hassan, 1981), also the study of water balance of
59 central part of Erbil basin by (Al-kubaisi et al, 2019). The study of water balance for Khanaqin
60 basin, east of Iraq by (Al-Sudani, 2018). Then the study on groundwater recharge was conducted
61 using meteorological water balance in khan area (Al-Sudani, 2018). As well as, another study on
62 Erbil basin groundwater recharge potential zone was used using fuzzy-Analytical Hierarchy Process
63 (AHP) in the north part of Iraq (Hamad, 2022). A study was being conducted on the impact of
64 climate change on the water balance of Erbil basin. Erbil basin was being faced with threats from

65 rising temperatures and shifting rainfall patterns due to global warming. To understand how these
66 climate shifts could affect the basin's hydrology, the water balance under current and projected
67 future climate scenarios was being modeled. Meteorological data such as precipitation, temperature,
68 humidity and wind speed over the past few decades had been collected and analyzed. (Nanakaley,
69 2019). A water balance was calculated for the period 2006-2021, using meteorological data from
70 Erbil station. Potential evapotranspiration was estimated at 1564.mm using the Thornthwaite
71 technique. The water surplus was determined to be 64.3 mm, and the water deficit was estimated to
72 be 1,848.7 mm. Annual surface runoff and recharge were determined to be, respectively, 46.97 mm
73 and 31.46 mm. The climate of the Erbil basin was concluded to be arid based on the results of the
74 water balance calculation. (Jalal, 2022). A study was conducted by (Hassan, 2022) on groundwater
75 modeling in the Kapran sub-basin under transient state flowconditions. MODFLOW was used to
76 predict groundwater conditions in 2039. The aquifer was modeled in an unconfined environment and
77 is represented by a single layer with thicknessesranging from 280m to 640m. The groundwater data
78 for period (2003-2021) was used for calibration of the model, the results of the model fits very well
79 with the observed data, then the model was run to predict the groundwater condition for the next 18
80 years (2021-2039). The result predicts 42m (2.33 m/year) ground water drawdown for the prediction
81 period. As well as, in the same study presents that the excessive exploitation of groundwater in the
82 Northern Erbil basin resulted in a (49.74m) drawdown across the study region from (2003 to 2021),
83 equivalent to (2.76 m/year) decline in groundwater, due to thousands of illegall wells drilled in the
84 study area. In general, large amounts of water were used without a defined policy for the use of
85 water resources and water sustainability. The lack of understanding among individuals and
86 institutions was found to have a substantial influence on groundwater depletion. The Erbil aquifer
87 will be depleted due to continuing negligence and recklessness in the usage of water resources. Then
88 the study of (Rafaat, 2023) was conducted who studied on Bastora catchment area that was located
89 in the northern part of Erbil basin, which has a semi-arid to arid climate condition, with cold and

90 rainy winters and hot and dry summers. Based on the Soil Conservation Service (SCS) method, the
91 surface runoff was determined to reach (195 mm/year) and the groundwater budget was calculated to
92 be (24.5 m³ /year). The soil type was classified as (type B) and the curve number was determined to
93 be (CN=72) according to the results of hydrological modelling. Based on the Horton model equation
94 and double ring methods, the infiltration rate was estimated to be 195.75 and 18.25 mm/hr
95 respectively. Rainfall is the only input element in the water balance, this element affects surface
96 runoff and groundwater recharge, representing the outputs of the water balance elements. The study
97 was limited due to the accuracy of the meteorological data, and monthly data was only obtained for
98 periods of (1995-2020), while more data could have provided a better estimation and prediction for
99 future aspects. Thus, due to the fact of increasing inhabitants during the last decades, and due to the
100 establishment of agricultural and industrial projects, groundwater utilization has become a vital
101 resource and alternative to surface water in the study area region.

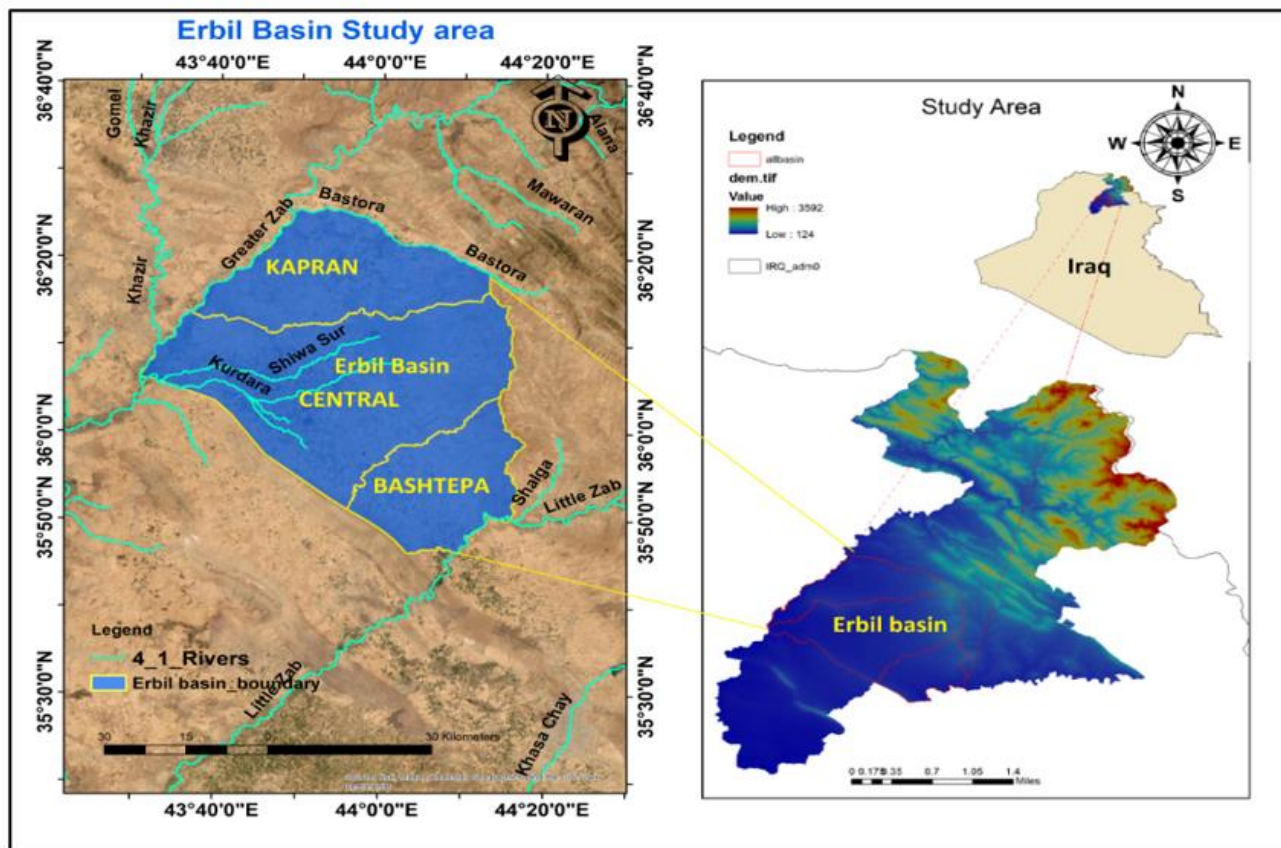
102 The main objective of this study was to determine the water budget of the Erbil groundwater
103 basin, which is very important for managing and keeping sustainability of water resources in the
104 region.

105 **2. Materials and methods**

106 *2.1. Locations of the Study area*

107 Erbil basin lies between latitudes (36° 08' 30" and 36° 14' 15") and Longitudes (43° 57' 30"
108 and 44° 03' 20"), The basin is naturally bordered by two rivers of Greater Zab and Lesser Zab
109 forming north and south respectively. From east and north-east, Pirman Dag was acting as a water
110 divide and the Kirkuk structure (Avana and Khurmala domes) restricted the area of study from west
111 and south-west representing the second water divide. The total area of the regional Erbil basin was
112 about (3,200 Km²) which was divided into three main parts according to groundwater flow. The first
113 part was the Kapran basin which was the northern part of Erbil basin, the second was the central part

114 basin which was the intermediate basin, and the third was Bashtepa which lay in the southern part of
 115 the Erbil basin (Hassan,1981), see Figure1:



116
 117 **Figure 1. Location of the study area, Erbil basin (Arc Map 10.8)**

118 *2.2. Hydrological conditions of the Study area*

119 The climate data of the Erbil meteorological station had been collected for the period (1995-2020)
 120 for this study. The sum and average amount of each parameters were tabulated in Table 1.

121 **Table 1: the climate data record in Erbil station for the period (1995-2020)**

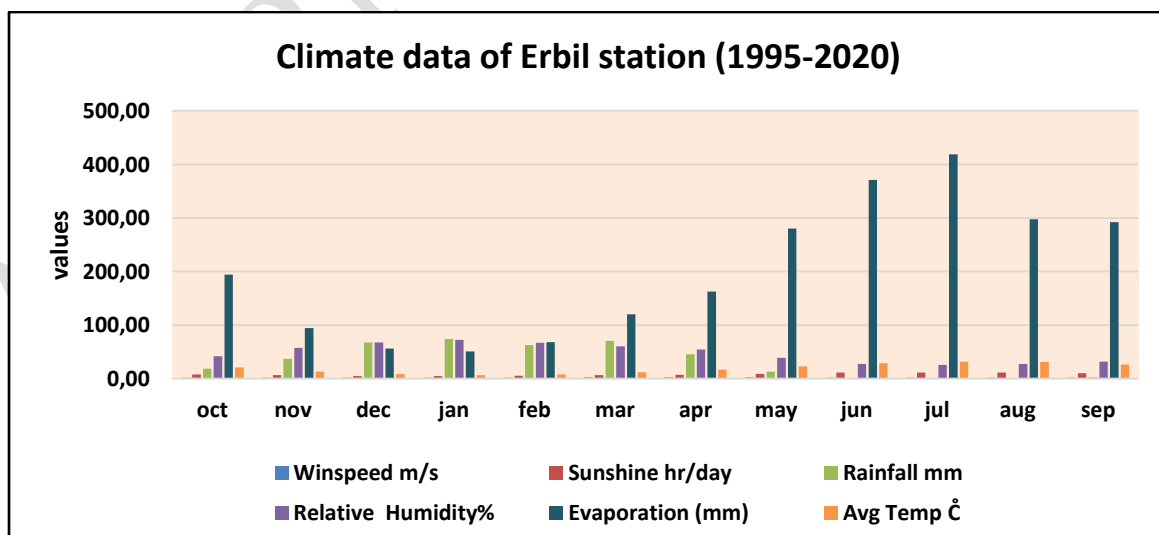
Erbil station data during (1995-2020)						
Month	Winspeed m/s	Sunshine hr/day	Rainfall mm	Relative Humidity%	Evaporation (mm)	Avg Temp °C
Oct	1.92	7.86	18.61	42.18	194.18	21.09

Nov	1.71	6.50	36.92	57.72	94.73	13.50
Dec	1.83	5.19	67.63	67.70	56.22	8.47
Jan	1.97	4.91	74.27	72.39	50.70	6.95
Feb	2.20	5.81	63.13	67.23	68.45	8.20
Mar	2.37	6.57	70.88	60.69	120.09	11.97
Apr	2.36	7.49	45.68	54.30	162.71	16.78
May	2.36	9.31	13.27	38.90	280.16	22.76
Jun	2.23	11.52	1.62	27.59	371.26	28.53
Jul	2.08	11.66	0.20	25.71	419.11	31.57
Aug	1.84	11.21	0.04	27.62	297.82	31.02
Sep	1.71	10.12	2.41	31.75	292.10	26.40
Sum	24.60	98.15	394.65	573.79	2407.53	227.24
Avg.	2.05	8.18	32.89	47.82	200.63	18.94

122

123 The chart of the climate data are shown in Figure 2:

124



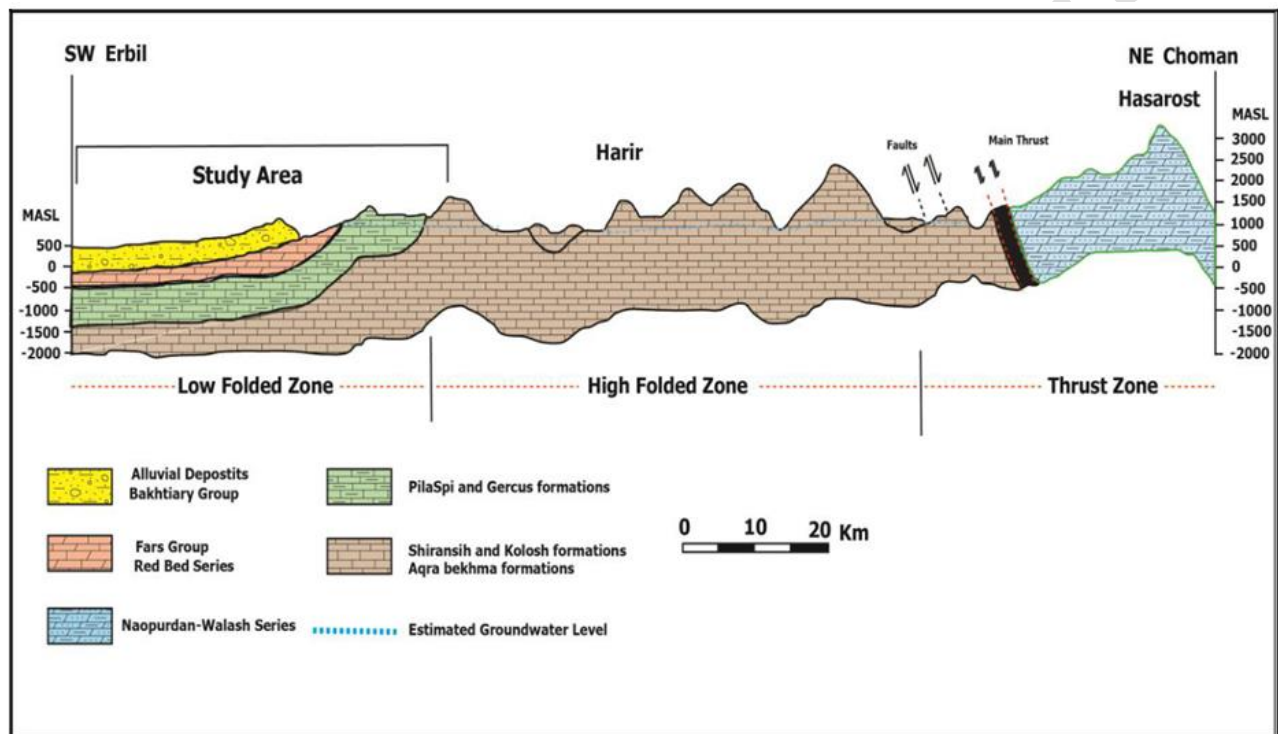
125

126

Figure 2. The climate data for the periods (1995-2020)

127 2.3. Hydrogeological conditions of the Study area

128 According to (Al Kubaisi, 2008) who indicated that the intervals of the trend of the center of the
129 depositional basin through Erbil basin had a thickness of about 3048 m. Also, the sediment was
130 composed of the (siltstone, sandstone, and conglomerate) this occurred during the upper Miocene,
131 Pliocene and Pleistocene, an uplift with intensive folding and thrusting and concurrent subsidence of
132 deep basins had occurred in North and North East of Iraq, see Figure 3:



133

134 **Figure 3. Regional hydrogeological cross section of Choman-Erbil (Dizayee, 2014)**

135 **3. Methodology and data analysis**

136 *3.1 Water budget component calculations*

137 The meteorological data obtained from Erbil station were analyzed to estimate the water budget and
138 characteristics of the selected region. In order to understand the hydrological conditions of the area.

139 The analysis began by calculating the average annual precipitation and converting the rainfall data
140 into a volume for the periods of (1995-2020), which gave the volume of precipitation over the basin.

141 Obtaining knowledge of the volume of precipitation over the basin was important. In fact, for the

142 Erbil Basin, the precipitation was the most crucial factor because it was the main source of the basin

143 recharge (Dizayee, 2014). However, the total amount of precipitation would not infiltrate into the
144 subsurface, some of the precipitation evaporated. The rest of the precipitation ran off the surface.
145 The calculations started by calculating the volume of precipitation over the basin. The water budget
146 equation was:

$$147 \text{ Inflow} - \text{Outflow} = \pm \text{change in storage} \quad (1)$$

$$148 \text{ Precipitation} - (\text{Evaporation} + \text{Recharge} + \text{Runoff}) = \pm \text{change in storage}$$

149 Precipitation

$$150 \text{ Volume of precipitation over the basin (m}^3\text{/year)} = \text{average annual precipitation (m/year)} \times \text{basin}$$

151 $\text{area (m}^2\text{)}$ (2)

$$152 \text{ Volume of precipitation over the basin (m}^3\text{/year)} = (0.39465 \text{ m/year}) \times \text{basin area (3,200,000,000}$$

153 $\text{m}^2\text{)}$ (The value of 0.39465 m/year estimated during the study for periods 1995-2020 which is from
154 meteorological data)

$$155 \text{ Volume of precipitation over the basin (m}^3\text{/year)} = 1,262,880,000 \text{ m}^3\text{/year}$$

156 Evaporation

157 Evaporation was one of an important element to estimate the water balance. However, evaporation
158 was is a variable element and depends on many factors, for instance temperature and humidity.
159 According to the climatic conditions in the study area, the best method to estimate evaporation was
160 called Ivanoff equation such as described in (Hassan ,1998):

$$161 E = 0.0018 (t+25)^2 (100-a) \quad (3)$$

162 Where:

163 E= monthly probable evaporation (mm)

164 t= mean monthly temperature (C°)

165 a= mean monthly relative humidity

166 Thus, the Ivanoff equation was used to calculate the average annual evaporation rates for each year
 167 based on the average annual temperature and precipitation which were calculated from the available
 168 climate data from Erbil meteorological station, Table 2:

169

170

Table 2. Evaporation calculation by Ivanof equation

Month	t	a	$0.0018(t+25)^2$	100 - a	Evaporation (mm)	P(mm)
Oct	21.09	42.18	3.8	57.8	221.1	18.61
Nov	13.50	57.72	2.7	42.3	112.8	36.92
Dec	8.47	67.70	2.0	32.3	65.1	67.63
Jan	6.95	72.39	1.8	27.6	50.8	74.27
Feb	8.20	67.23	2.0	32.8	65.0	63.13
Mar	11.97	60.69	2.5	39.3	96.7	70.88
Apr	16.78	54.30	3.1	45.7	143.5	45.68
May	22.76	38.90	4.1	61.1	250.9	13.27
Jun	28.53	27.59	5.2	72.4	373.5	1.62
Jul	31.57	25.71	5.8	74.3	427.9	0.20
Aug	31.02	27.62	5.6	72.4	408.9	0.04
Sep	26.40	31.75	4.8	68.2	324.6	2.41
sum					2540.7	394.65
Avg.					211.7	
				Evaporation	54%	

171

172 The volume of evaporation over the basin is calculated by:

173 Volume of Evaporation over the basin (m^3/year) = average annual evaporation (m/year) X
174 basin area (m^2) (3)

175 The results of the calculations show that the average volume of evaporation over the basin is
176 (681,955,200) m^3/year , which is (54%) of the total precipitation.

ACCEPTED MANUSCRIPT

177 Recharge

178 The calculation of the evaporation was not involved in the whole calculations for estimating the
179 water balance because a constant rate of 24.23% of precipitation infiltrated into the subsurface. The
180 main source of recharge in the Erbil Basin was precipitation. The recharge rate to unconfined
181 aquifers from precipitation was 24.23% (Hassan, 1998). Thus, from infiltration (groundwater
182 recharge) and evaporation rates the Run off in Erbil Basin could be calculated as follows:

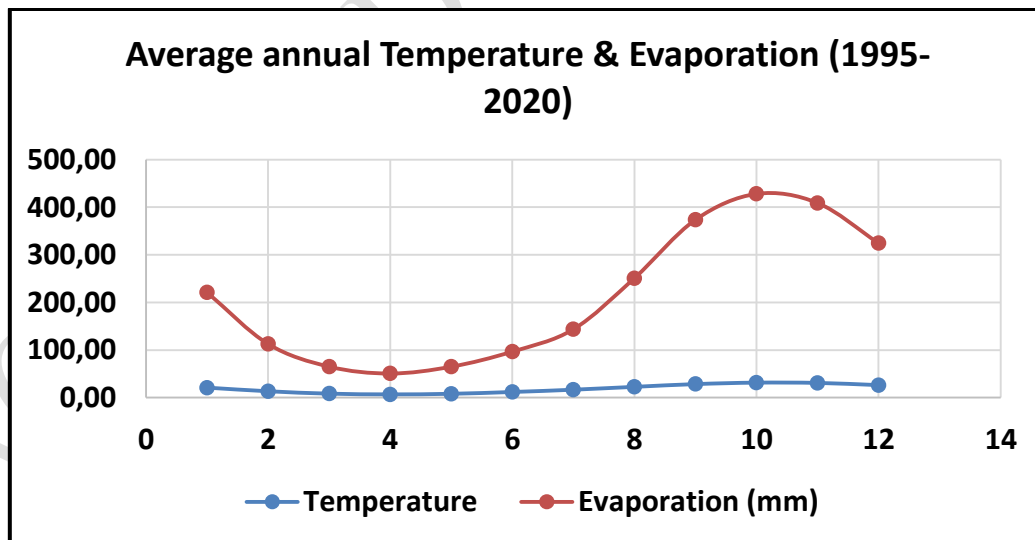
183 Average Runoff = Average annual precipitation (100%) – Infiltration rate (24.23 %) – Evaporation
184 rate (55%) (4)

185 Average Runoff = 100 % - 24.23% - 54%

186 Average Runoff = 21.77 %

187 This calculation shows that 21.77% is surface Runoff. therefore, the total amount of precipitation
188 54% evaporates, 24.23% infiltrates into the groundwater to be recharge. To show the relation
189 between Temperature and evaporations see Figure 4:

190



191

192 **Figure 4. The Relation between average annual temperature and average annual**
193 **evaporation in the study area.**

194

195 To calculate the sustainable water use (pumping) in the Erbil Basin, the researcher calculated

196 the average annual recharge as follow:

197 Average annual recharge (m^3/year) = (Volume of precipitation over the basin (m^3/year) X
198 infiltration rate %) / 100 (5)

199 Average annual recharge (m^3/year) = 1,262,880,000 m^3/year X 0.2423

200 Average annual recharge (m^3/year) = 305,995,824 m^3/year

201 The amount of groundwater decline in Erbil three sub-basins are calculated as shown in Table 3:

202 **Table 3 groundwater decline during (2004-2023) in Erbil three sub-basins**

Sub-basin	2004-2023	Area (m^2)
Northern (Kapran)	-33	772,000,000
Central	-51	1,742,000,000
Southern (Bashtepa)	-55	585,000,000
Average	-46.3	(-) means decline in groundwater
decline per 18 years	-2.57	

203 Table 3 showed the water level decline in each sub-basin, 33 meters, 51 meters, and 55 meters
204 decline in Kapran, Central, and Bashtepa sub-basins respectively. The decline in the water table,
205 based on the (55) wells that had been used as monitoring groundwater and had repeated water
206 levels data recorded, was 2.57 m/year. This decline in groundwater was mainly due to a cluster of
207 wells in each sub-basin, where the number of wells exceeded the legally permitted numbers. To
208 estimate the accurate results on the groundwater conditions in the Erbil Basin, the volume of the
209 annual water use in the basin was calculated as follows:

210 Volume of the annual water use (m^3/year) = Average annual decline in the basin (m/year) X
211 basin area (m^2)

212 (6)

213 Volume of the annual water use (m^3/year) = 2.46 m/year * 3,200,000,000 m^2

214 Volume of the annual water use (m^3/year) = 7,872,000,000 m^3/year

215 This number helps characterize the volume of water being overexploited in the region as below:

216 Volume of overexploitation (m^3/year) = Volume of water used (m^3/year) – Recharge volume

217 (m^3/year) (7)

218 Volume of overexploitation (m^3/year) = 7,872,000,000 - 305,995,824

219 Volume of overexploitation (m^3/year) = 7,580,008,352 m^3/year

220 To estimate the total water being pumped by the recharge using the following calculation:

221 Amount of pumped water that is recharged by precipitation = (Recharge volume / volume of water

222 used)* 100 (8)

223 Amount of pumped water that is recharged by precipitation = (305,995,824/ 7,872,000,000)* 100

224 Amount of pumped water that is recharged by precipitation = 4%

225 To reach to sustainability, the recharge will need to increase by (96%). The sustainable recovery

226 pumping rate is then calculated by:

227 Sustainable Recovery pumping m^3/year = Volume of average annual recharge m^3/year *

228 90%(9)

229 Sustainable Recovery pumping (m^3/year) = 305,995,824*90%

230 The results of this calculation indicate that, in order to keep 10% of the recharge in the basin for

231 the purpose of basin recovery, the sustainable pumping of the groundwater from the Erbil Basin

232 is 275,396,241.6 m^3/year .

233

234 **Table 4. Results of the water budget elements calculations**

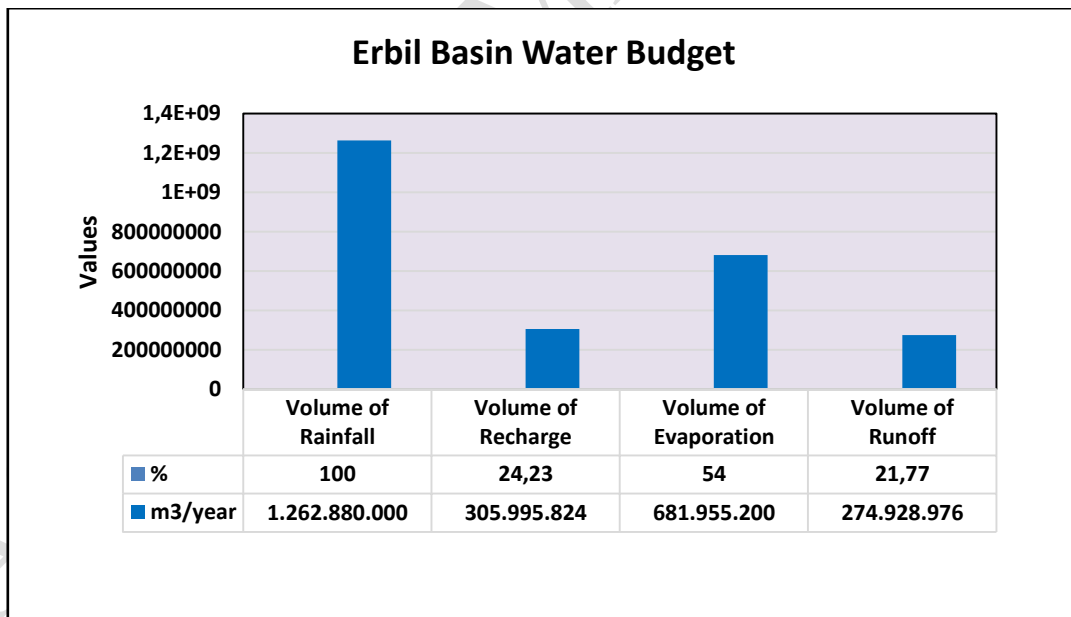
Average annual precipitation (m)	0.39465
Basin area (m^2)	3,200,000,000
Volume of precipitation over the basin (m^3/year)	1,262,880,000
Recharge volume (m^3/year) based on 24.23% (Hassan)	305,995,824
Water table decline (m/year) as measured in 55 wells	2.57
Volume of annual water use (m^3/year) based on 2.56 m/year decline	8,192,000,000

volume of overexploitation (m ³ /year) based on 2.56 m/year decline	7,886,004,176
Water table decline (m/year) (based on 18 years decline in water table)	2.57
Water table decline (m/year) based on calculated overexploitation	2.46
Volume of annual water use (m ³ /year)	7,872,004,000
Volume of overexploitation (m ³ /year)	7,580,008,352
Water table decline – Recharge volume	(96% of total use is overexploitation)
Total of the pumped water met by recharge	4%
Volume of Evaporation (m ³ /year) (54% of total precipitation)	681,955,200

235

236 The values of each elements of water budget are plotted in Figure 5:

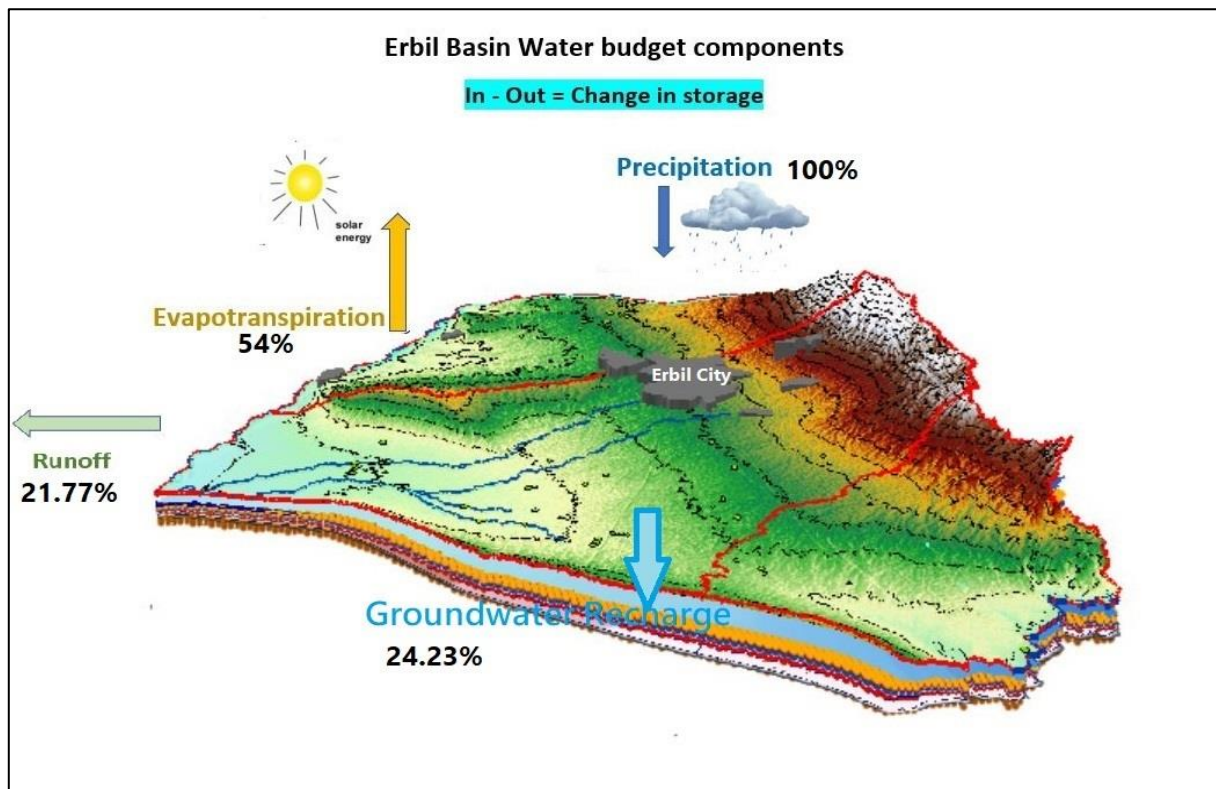
237



238

239

Figure 5. Values of estimated water budget



240

241

Figure 6. Erbil basin water budget estimation

242

243 3.2 Population characteristics and assessment of water budget

244 The number of populations in study area in (1977) is (266,650), which comprises (65.9%) of total
 245 percentage of Erbil governorate populations. The population in Erbil basin in (2004) is (886,585)
 246 citizens however, in (2009) it is (1,173,036) based on the study of (Ahmad, 2012), see Table 5:

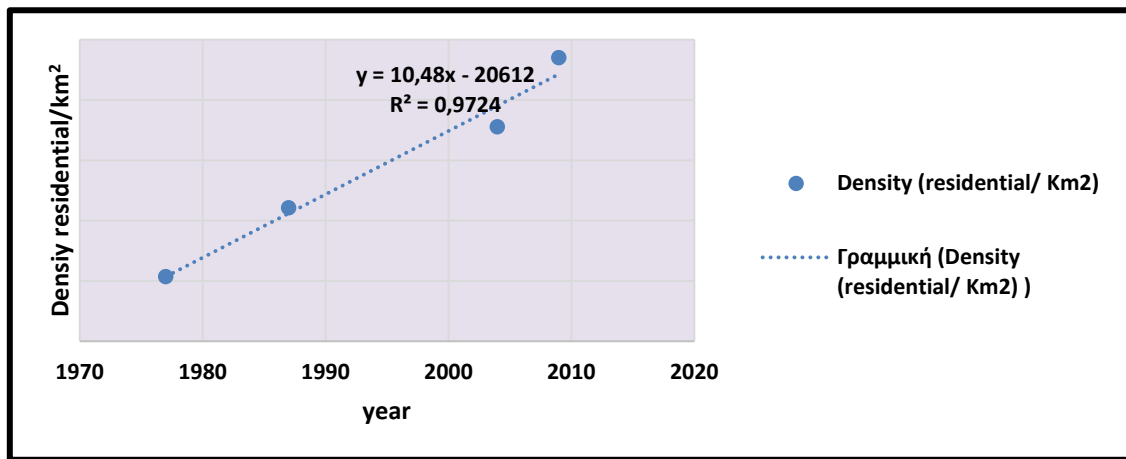
247

Table 5. density of residential for years (1977-2009) (Ahmad, 2012)

Year	Population	Density (residential/ Km ²)
1977	266,650	107
1987	553,038	221
2004	886,585	355
2009	1,173,036	470

248

249 The relationships between the values of each year are plotted in Figure 7:



250
251 **Figure 7. Residential density versus year in the study area**

252 In addition, to estimate water demand for Erbil basin, the number of the population needed to be
253 known. In order to determine the annual increment ratio, the following formula which was
254 described in (Hassan, 1998) was used:

255
$$r = \frac{1}{n} \left(\frac{P_n}{P_0} - 1 \right) \quad (10)$$

256 Where:

257 r: annual increment ratio

258 P_n : population number in a given statistical encountering

259 P_0 : population number in prior statistical encountering

260 n: Number of years between the two encountering

261
$$r = \frac{1}{5} \left(\frac{1,173,036}{886,585} - 1 \right)$$

262 $r = 0.065$

263 In order to determine the number of populations in any time use the equation below:

264
$$P_t = P_0 (1 + r t) \quad (11)$$

265 Where:

266 P_t : population number at any year in the future

267 P_0 : population number at a known year

268 r: population increment ratio

269 t: Number of years between P_0 and P_t

270 Thus, to determine population in (2023) based on year 2009 it is as follow:

271 $P_t = P_o (1 + r t)$

272 $P_{2023} = 1,173,036 (1 + 0.065 (14))$

273 $P_{2023} = 2,240,499$ citizens

274 Average daily water consumption in Erbil City was about 380 liters/Capita/day based on the data
275 obtained from the Directorate of Water and Sewerage in the Kurdistan Region of Iraq (2023). The
276 estimated water demand for the future long term was as shown in Table 6:

277 **Table 6. estimation water demand for each year**

Year	Initial P values	demand m ³ /year
2023	P ₂₀₀₉ =1,173,036	P ₂₀₂₃ =310,757,178
2030		P ₂₀₃₀ =384,785,720.4
2040		P ₂₀₄₀ =490,540,781
2050		P ₂₀₅₀ =596,295,841.6

278
279 Water based on the data available, the number of wells were about 8,342 wells based on data taken
280 from the General Directorate of Water and Sewerage in the Kurdistan Region of Iraq (2023).

281 The estimated rate of well drainage for each well =25 m³/hr.

282 The average number of operating hours for each well =15 hours.

283 The produced water from wells =8,342 wells (legal and recorded wells within Erbil basin)

284 The total quantity of water= Water treatment plants + groundwater wells

285 $WTP = 34,000 + 44,000 + 216,000 = 294,000 \text{ m}^3/\text{day}$

286 $\text{Groundwater wells} = 8,342 \text{ wells} \times 15 \text{ hr} \times 25 \text{ m}^3/\text{hr} = 3,128,250 \text{ m}^3/\text{day}$

287 $294,000 + 3,128,250 = 3,422,250 \text{ m}^3/\text{day}$

288 The rate of loss is about 15% (General Directorate of Water and Sewerage in the Kurdistan region
289 of Iraq, 2023).

290 Thus, the remaining net quantity = $3,422,250 \times 85 \% = 2,908,913 \text{ m}^3/\text{day}$.

291 Annual water consumption = $2,908,913 \text{ m}^3/\text{day} \times 365 \text{ day}$

292 = $1,061,753,063 \text{ m}^3/\text{year}$.

293 Thus, the lack of water supply in the Erbil Basin is water demand minus water consumption

294 = $310,757,178 - 1,061,753,063$

295 = $-750,995,885 \text{ m}^3/\text{year}$ as the required amount of water (2023)

296 The negative sign indicates that there is lack of water demand.

297 3.3 Groundwater Modeling approach

298 The study also estimate the sentivity analysis of the groundwater modeling. Groundwater modeling

299 was used to estimate the water budget for Erbil basin. A three-dimensional groundwater flow model

300 was developed using MODFLOW software. The model incorporated the geology and hydrogeology

301 of the basin based on available data such as lithology, stratigraphy, structural features, aquifer

302 parameters, recharge rates, etc. The model domain was discretized into grid cells and layers to

303 represent the subsurface geology. Relevant hydrological processes like groundwater recharge,

304 discharge, flow and storage were programmed into the model. The model was calibrated by

305 adjusting model inputs until the simulated groundwater heads matched observed field

306 measurements within an acceptable error range. Once calibrated, the model was used to simulate

307 groundwater flow over time under historic pumping and recharge conditions. Key outputs of the

308 model like annual groundwater recharge, discharge, storage changes and flows across boundaries

309 were used to calculate the different components of the water budget for Erbil basin. The

310 groundwater modeling approach provided a quantitative estimate of the basin-scale water budget

311 (Al-Areedhi, 2019), see Figure 8:

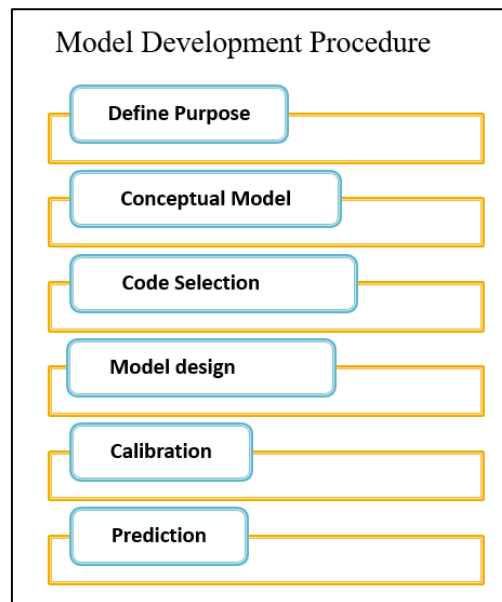


Figure 8. Flow chart of the study and GMS applications

312

313

314

315 In this study, the equation of steady-state heterogeneous and an isotropic is applied for the
 316 application of GMS software version 10.7. The methodology of this study can be started from
 317 collecting the data on the investigated area, which was provided by the General Directorate of Erbil
 318 groundwater and General Directorate of Water Resources, the collected information includes well
 319 data, topographic maps, number of the existing wells, and hydrogeological data. Then the raw data
 320 prepared by GIS program to be ready to input into (GMS) software for building Conceptual model.
 321 The GMS is used to simulate the steady states groundwater flow conditions using the solver
 322 package MODFLOW 2000 based on finite difference techniques (Al-Areedhi and Khayyun, 2019).

$$323 \quad \frac{\partial}{\partial x} \left(Kx \frac{\partial h}{\partial x} \right) + \frac{\partial}{\partial y} \left(Ky \frac{\partial h}{\partial y} \right) + \frac{\partial}{\partial z} \left(Kz \frac{\partial h}{\partial z} \right) = 0 \quad (12)$$

324 Where:

325 K: is hydraulic conductivity (LT^{-1}) in (x,y,z) directions.

326 h: is hydraulic head (L).

327 3.3.1 Building conceptual model

328 Building a conceptual model in GMS is a methodical procedure aimed at creating a comprehensive
 329 representation of the hydrogeologic conditions in a study area (Al-Areedhi and Khayyun, 2019).

330 The process commences with the input of model boundary files into the map data coverage,
331 defining the spatial extent of the model area. Following this, the coverage is enriched by
332 incorporating data pertaining to wells and observation head locations, crucial components that
333 contribute valuable information to the model. Wells play a significant role in representing points of
334 water extraction or injection, while observation heads serve to capture groundwater elevation data.
335 In addition to these components, an additional layer is introduced to the conceptual model through a
336 coverage that outlines boundary conditions. This layer is essential for specifying sources and sinks
337 within the groundwater system, providing a framework to simulate the dynamic interactions
338 influencing groundwater movement. Through the systematic integration of these components, the
339 conceptual model in GMS becomes a powerful tool for accurately simulating and understanding the
340 hydrogeologic complexities of the study area.

341 *3.3.2 Model grid and setting boundary condition*

342 Once the conceptual model is established, the next step involves the creation of a 3D grid structure
343 in GMS. This is accomplished by selecting new and then 3D Grid, followed by assigning boundary
344 conditions in alignment with the nature of the Erbil Basin. Given the geographical limitations posed
345 by the Greater Zab and Lesser Zab Rivers, the boundary conditions are carefully defined to
346 encapsulate the hydrogeologic characteristics of the region. For the river boundaries, the
347 MODFLOW 2000 Grid utilizes the river package, incorporating the specific features of the river
348 sides into the model. Additionally, locations corresponding to groundwater divides, marked by the
349 outcrops of geological formations, are designated as no-flow boundary conditions. The head inside
350 the model represents the groundwater head, effectively mirroring the groundwater table observed in
351 existing wells. Figure 9 illustrates the 3D grid structure of the model, providing a visual
352 representation of the aquifer types and their spatial arrangement within the Erbil Basin. In addition,
353 the detail about assigning the input data are summarized in Table 7.

354 **Table 7.** input data for MODFLOW 2000 package in GMS software

Conceptual model	Descriptions of the items
Model domain	Cell sizes (100 by 100) m by 700 m depth of the aquifer
Boundary condition	River conductance (2.74 and 2.29) m ² /d/m for Greater and lesser Zab rivers respectively
	Greater Zab River U/S node GZ= (279 m and 277m) and D/S node GZ= (215 m and 213 m) Lesser Zab River U/S node LZ= (270 m and 268m) and D/S node LZ= (252 m and 250 m)
Aquifer types coverage	Define each of the material's hydraulic conductivity in LPF package
Recharge Coverage (RCH)	The polygon of the model area defined by (RCH=0.000385 m/day) as initial values including (10%-40% Avegarge annual rainfall) + surface water bodies
Existing wells coverage	Number of the wells (8384 wells) + (55 observation wells)

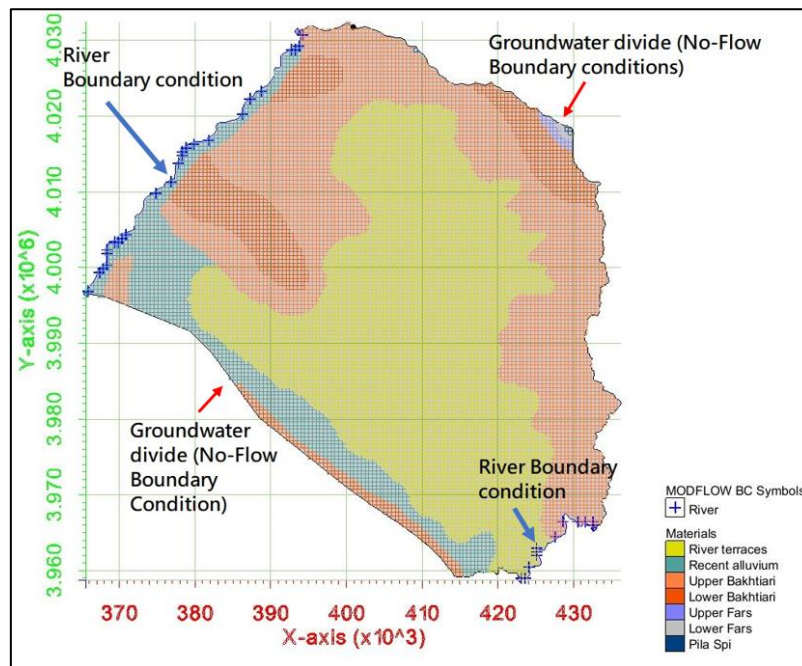
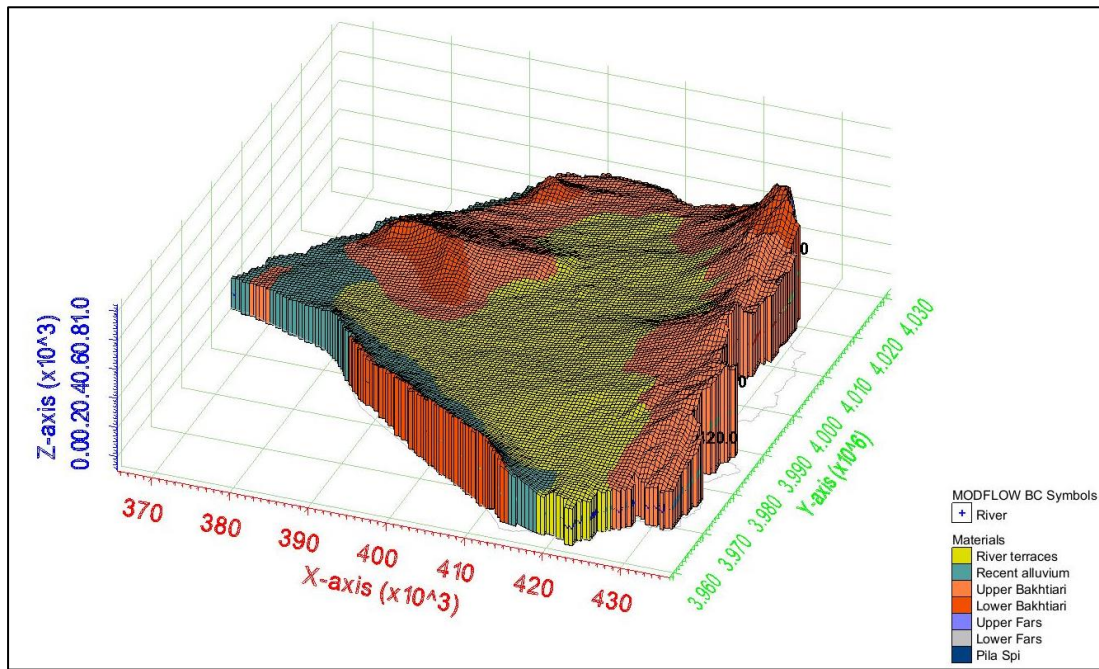


Figure 9. The boundary conditions used in the study.

3.3.3 Create new simulation (MODFLOW) steady-state conditions

The transition from the conceptual model to the MODFLOW simulation involves a critical step of mapping the relevant parameters. This process includes the interpolation of the top and bottom of the model layer onto the 3D grid. All coverages in the conceptual model are converted using the map to MODFLOW tool, facilitating a seamless integration of the conceptual model into the numerical simulation. The top of the model grid corresponds to the natural groundwater surface, represented by a Digital Elevation Model (DEM) with a resolution of cell sizes set at (28 x 28) meters. This DEM essentially serves as a topographic map of the Erbil Basin, providing a precise depiction of the surface elevation. Notably, the bottom of the 3D grid aligns with the depth of the drilled wells, capturing the subsurface configuration (Al-Areedhi and Khayyun, 2019). The model, showcased in Figure 10, effectively delineates the characteristics of the unconfined aquifer types within the Erbil Basin, emphasizing the importance of accurate mapping for a comprehensive representation in groundwater simulations. In addition, based on the formation types within Erbil basin, the values of the Hydraulic conductivity obtained from the following Table 8.



372

373

Figure 10. the Model structure of the Aquifer types (geological formations).

374

375

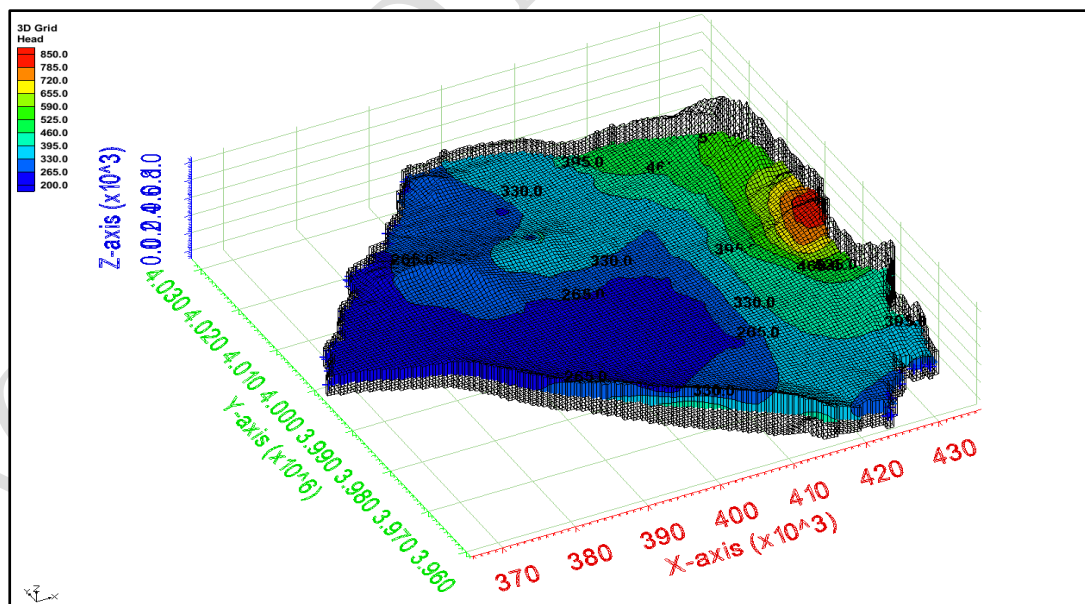
Table 9. The Hydraulic conductivity ranges (Freeze and Cherry, 1979).

Descriptions of the rock types	K min (m/day)	K max (m/day)
Unconsolidated deposits		
Coarse gravel	864	8640
Sands and gravels	0.864	864
Fine sands, silts	0.0000864	0.864
Clay, shale, glacial	8.64E-09	0.0000864
Hard rocks		
Dolomitic limestone	0.864	86.4
Weathered chalk	0.864	86.4
Limestone	0.0000864	0.0864
Sandstone	0.00000864	8.64
Granite, Gneis, Compact basalt	8.64E-09	0.0000864

376

377 3.3.4 Run steady-state model

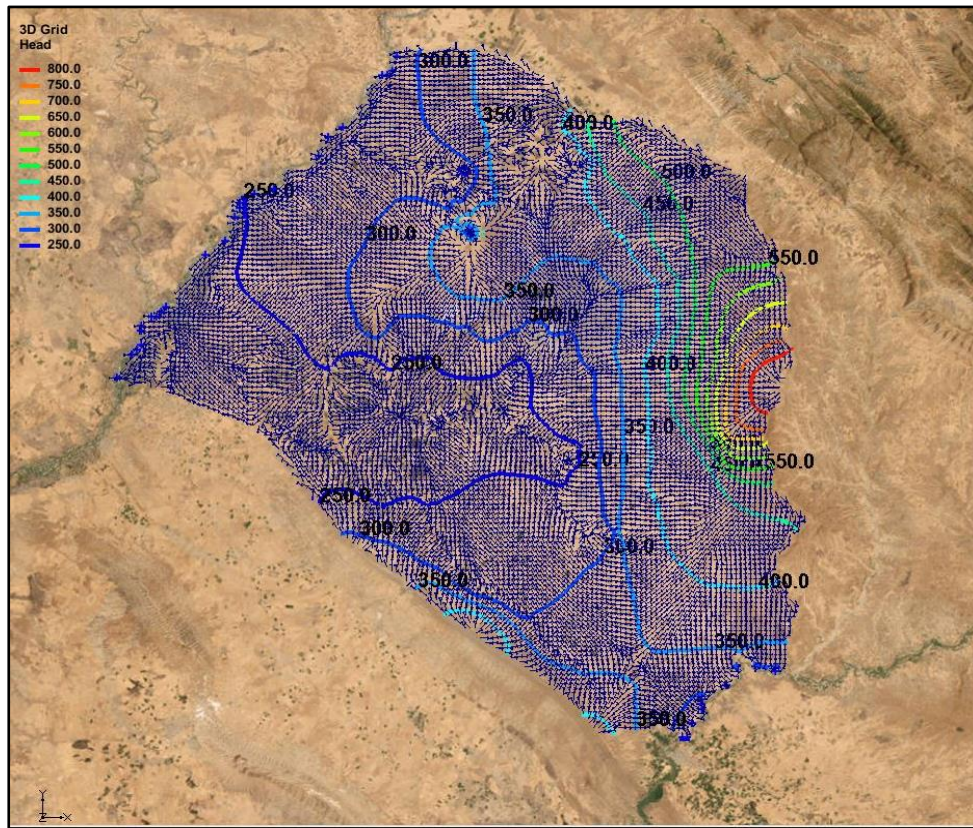
378 The calibration process in groundwater modeling involves adjusting model parameters to align
379 calculated results with observed hydraulic patterns of groundwater flow. This adaptation is crucial
380 for ensuring that the model accurately represents the real-world behavior of the aquifer system. Key
381 elements in the calibration process include measured head values and local flow directions, often
382 derived from interpolations of head measurements to create contour lines of the groundwater
383 surface (McDonald, et al., 1988). In the case of the Erbil model, the flow direction and associated
384 heads are intricately linked to the morphology of the layered aquifers. Despite the presence of a
385 significant number of observation wells distributed across the model domain, common interpolation
386 methods prove to be challenging in accurately representing water table characteristics due to the
387 complex nature of the aquifer system. The limitations of these methods are highlighted in Figure 11,
388 underscoring the need for a thoughtful and context-specific calibration approach in capturing the
389 nuances of groundwater flow in the Erbil Basin. Whereas, the velocity vector obtained from the
390 model results are Figure 12.



391

392

Figure 11. The contour map of groundwater flow head



393

394

Figure 12. Distribution of the velocity vector over the model area

395

3.3.5 Calibration steady-state model using PEST pilot points

396

The primary objective of model calibration is to reduce the disparity between observed and

397

simulated head values by fine-tuning model parameters. Achieving this alignment is crucial for

398

ensuring that the model accurately reflects the actual behavior of the groundwater system.

399

Calibration can be carried out through manual adjustments via trial and error, or more

400

systematically through automated approaches like parameter estimation using PEST pilot points in

401

GMS. The effectiveness of calibration relies on the thorough characterization of field conditions at

402

the site (Al-Areedhi and Khayyun, 2019). Proper understanding and representation of the

403

hydrogeologic setting are essential for refining model parameters to attain an accurate simulation. In

404

the Erbil model, the results of the calibration process demonstrate a harmonious match between

405

observed and simulated head values, as depicted in Figure 13, indicating the success of the

406

calibration in capturing the intricacies of the groundwater flow in the studied area.

407 Following the model run, it is common for the obtained results to exhibit variations from the actual
408 field values. This disparity is inherent in modeling, given that it involves simplifications of the
409 complex physical behaviors of reality, and allowances are made for approximations and
410 computational errors. The critical step of model calibration is undertaken to minimize these
411 differences and align the model results with the actual field values (Al-Areedhi and Khayyun,
412 2019). In groundwater modeling, achieving concordance between the resulting observed head and
413 the simulated head at corresponding points is essential. This calibration process involves adjusting
414 model parameters, such as hydraulic conductivity (HK) or recharge (RCH), to optimize the match
415 between the model's predictions and the observed field data. Through a systematic adjustment of
416 these parameters, the calibration process seeks to enhance the model's accuracy, ensuring that it
417 captures the nuances of the groundwater flow in the studied area.

418 The calibration process is very important to represent the actual behavior of the model. To perform
419 this process, consider the observed groundwater head as $(h_{observed})_i$ at the observation point (i),
420 and the calculated head at the same point is $(h_{simulated})_i$, The root mean square error (RMSE)
421 equations are:

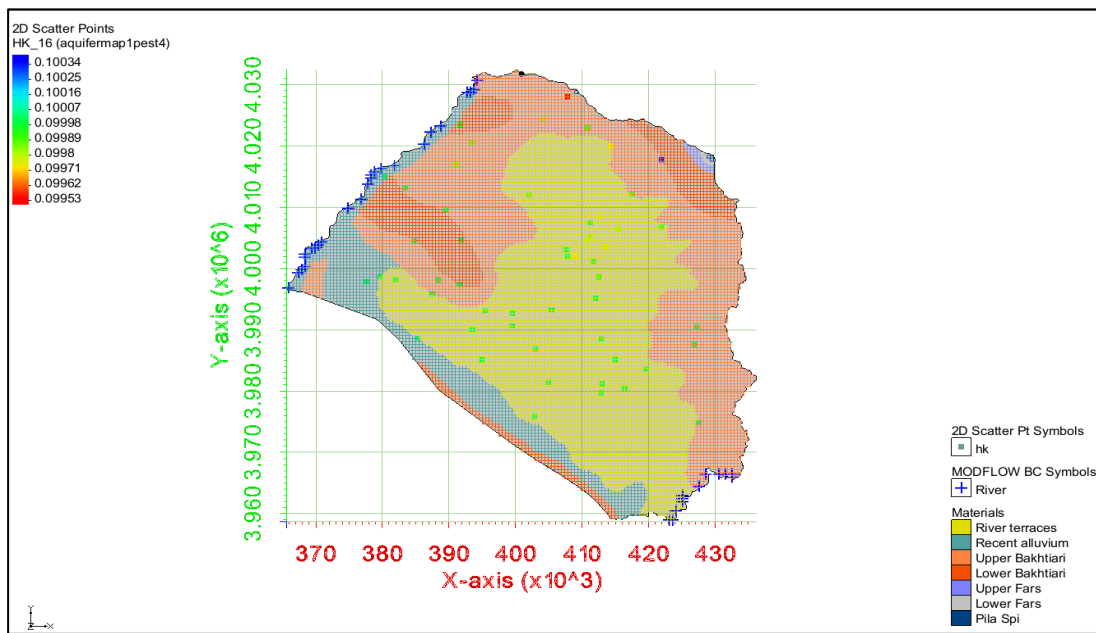
422 Mean Error equation: $ME = \frac{1}{2} \sum_{i=1}^n (h_{observed} - h_{simulated})_i$ (13)

423 Mean Absolute Error: $MAE = \frac{1}{2} \sum_{i=1}^n |h_{observed} - h_{simulated}|_i$ (14)

424 Root Mean Square Error: $RMSE = \sqrt{\frac{1}{2} \sum_{i=1}^n (h_{observed} - h_{simulated})_i^2}$ (15)

425
426 The final step in the groundwater modeling process is model validation, which occurs subsequent
427 to the calibration phase. The primary objective of model validation is to assess the general
428 performance of the calibrated model on datasets distinct from those used in the calibration process.
429 Calibration involves adjusting various parameters, such as hydraulic conductivity (HK) and
430 recharge (RCH), and different combinations of values can yield similar solutions. The validation
431 process is crucial in determining the broader applicability of the calibrated model beyond the

432 specific dataset used for calibration (MacDonald et al., 1988; Anderson et al., 2015; Al-Areedhi
433 and Khayyun, 2019). Typically, modelers divide the acquired data into two sets: one for calibration
434 and another for the validation process. By employing independent datasets for validation, modelers
435 can rigorously assess the model's robustness and reliability, ensuring that it provides accurate and
436 consistent results across different conditions. See Figure 14.



437

438 **Figure 14.** The 2D scatter points in the active grid for calibration PEST Pilot points

439

439 In this study, the minimization of errors in the groundwater model was achieved through the
440 application of PEST pilot points, particularly for hydraulic conductivity values sourced from
441 various pumping test results. PEST, a widely used parameter estimation tool, allows for a
442 systematic adjustment of model parameters to optimize the agreement between simulated and
443 observed data. By incorporating data from pumping tests and leveraging PEST pilot points, the
444 study aimed to enhance the accuracy of hydraulic conductivity values in the calibrated model.

445

445 The results of this application of PEST, which encapsulate the refined hydraulic conductivity
446 values, are succinctly summarized in Table 10. This table serves as a comprehensive compilation
447 of the outcomes of the parameter estimation process, providing a clear representation of the
448 adjusted model parameters achieved through the iterative application of PEST methodology.

449

449

450

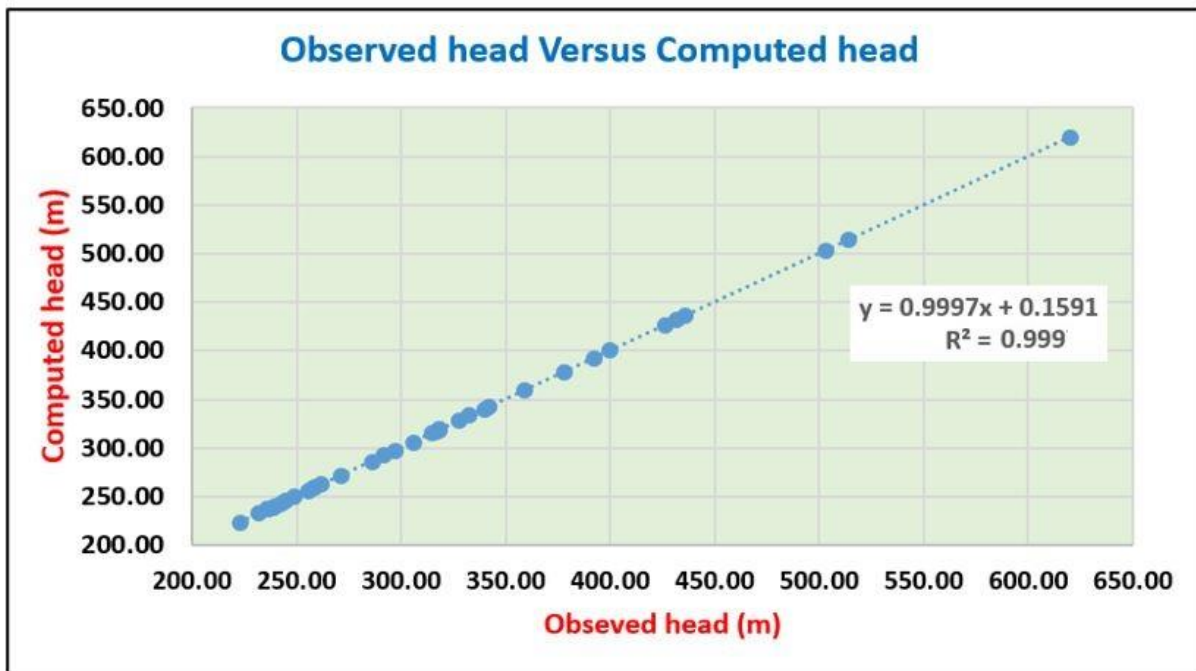
Table 10. The values of Errors in PEST application

Descriptions	Symbol	Values
Mean Residual (Head)	ME	-0.03
Mean Absolute Residual (Head)	MAE	0.24
Root Mean Squared Residual (Head)	RMSE	0.36

451

452 The Figure 15 depicts a comparison between computed and observed head values derived from the
453 model results. This graphical representation provides a visual assessment of the accuracy and
454 agreement between the simulated groundwater levels produced by the model and the actual
455 observed head values from the field. Analyzing the relationship between computed and observed
456 head values is crucial for evaluating the model's performance and its ability to replicate real-world
457 hydrogeologic conditions. The closer the points align to the line in the Figure 15, the better the
458 model's predictive capability, indicating a successful calibration and validation process.

459



460

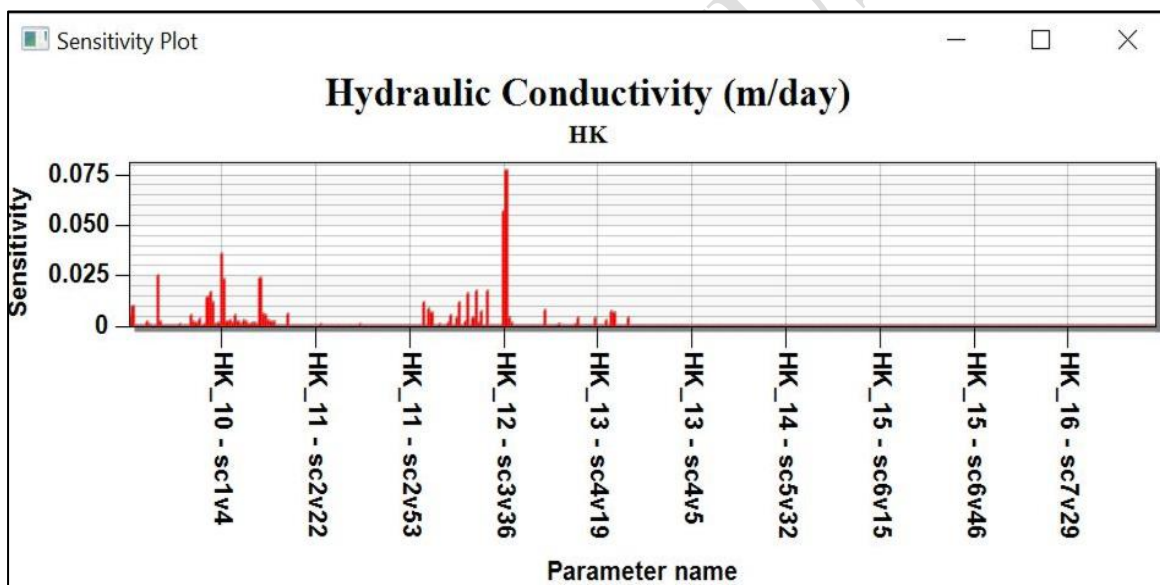
461

Figure 15. Plot of the observed head versus simulated head.

462

463 3.3.6 Sensitivity analysis

464 The sensitivity analysis is performed to compare between model results and parameters for case of
465 before and future periods of the calibration. It can be determined by fixing all the calibrated
466 parameters except of the selected parameter, this indicates which parameters have greater impact
467 on the model results. Parameters have high impact on the model results should get the most
468 attention in the calibration process and data collection. In addition, the most common method of
469 sensitivity analysis is the use of finite difference methods to estimate the rate of change in model
470 results due to change in the parameter (Mac Donald et al., 1988; Anderson et al., 2015; Al-Areedhi
471 and Khayyun, 2019). This study used the trial and error methods, then Automated Parameter
472 Estimation (PEST) and PEST Pilot points to optimize the parameter values as shown in Figure 16.



473
474 **Figure 16.** Parameter Sensitivity of the Hydraulic conductivity values used for PEST pilot
475 points.

476 3.3.7 Water Budget

477 The water budget analysis is a pivotal aspect of understanding the hydrologic dynamics within the
478 modeled region. In this study, the GMS software facilitated the computation of water budget
479 results, shedding light on the inflow and outflow components in the model. The quantity of
480 recharge, representing water inflow, is a critical parameter that influences the groundwater
481 system's sustainability. Concurrently, the outflow is determined by considering factors such as

482 production water wells and rivers, representing losses from the system. The GMS output provides
 483 a comprehensive overview of the water budget, encapsulating the intricate balance between inflow
 484 and outflow in the model region. The results, as summarized in Table 11, offer valuable insights
 485 into the overall water dynamics, enabling a nuanced understanding of the groundwater movement
 486 and sustainability within the studied area. This information is crucial for effective water resource
 487 management and informs decision-making processes related to the sustainable use of groundwater
 488 in the region.

489 **Table 11.** Water budget information obtained from steady state Run in GMS

	Flow In	Flow Out
Sources/Sinks		
Constant Head	0	0
Wells	0	-963,959.40
River Leakage	0	-194,677.92
Recharge	1,158,637.37	0
Total Source/Sink	1,158,637.37	-1,158,637.32
Zone Flow		
Flow Right Face	0	0
Flow Front Face	0	0
Flow Left Face	0	0
Flow Back Face	0	0
Total Zone Flow	0	0
Total Flow	1,158,637.37	-1,158,637.32
Summary	In - Out	% difference
Sources/Sinks	0.050743103	4.38E-06
Cell to Cell	0	0
Total	0.050743103	4.38E-06

490
 491 Table 11 provides a comprehensive breakdown of the water budget for the Erbil basin, offering
 492 valuable insights into the quantity of water entering and leaving the aquifer. This data holds
 493 significant importance for local authorities as it forms the cornerstone for informed decision-
 494 making regarding water resource management. Understanding the dynamics of water inflow,
 495 represented by recharge, and outflow, including water extracted from production wells and
 496 contributions from rivers, is crucial for ensuring the sustainability of this vital resource. The

497 information presented in the table serves as a foundational tool for authorities to plan and
498 implement measures that will safeguard the groundwater reserves for future generations. In regions
499 prone to drought problems, such as the Erbil area, this data-driven approach becomes even more
500 critical. It equips authorities with the knowledge needed to address challenges related to water
501 scarcity, enabling the formulation of strategic and sustainable solutions to mitigate the impact of
502 drought and secure a resilient water supply for the community.

503

504 **4. Results and Discussion**

505 The results of this study showed that the groundwater declined during the periods of (2004-2023),
506 and this decline was calculated by adding the average decline in each sub-basin and dividing the
507 result by three, so this gave the average decline in 18 years, dividing it by 18 gave the average
508 decline in a year. Multiplying the 2.57 m/year decline by the basin area gave the average volume of
509 annual water used in the basin, which was 8,192,000,000 m³/year. The annual water use volume
510 subtracted from the recharge volume (310,757,178 m³/year) gave overexploitation volume in the
511 basin, which was (7,886,004,176) m³/year. Dividing the volume of average annual overexploitation
512 (2,185,833,980 m³/ year) by the basin area gave 2.46 m/year water table decline due to
513 overexploitation in the basin. All of the calculations were based on a 2.46 m/year decline. To
514 double check it, the volume of annual water use and overexploitation were recalculated based on a
515 2.46 m/year decline. The sustainable pumping volume for the basin was equal to the average annual
516 recharge of the basin, which was (310,757,178 m³/ year). This volume represented what should be
517 extracted from the Erbil Basin instead of (7,580,008,352 m³/year). Furthermore, because the
518 groundwater levels in Erbil Basin were facing a serious depletion, the author also calculated a
519 recovery pumping rate, which required that a portion of the average annual recharge would not be
520 pumped from the basin so that the basin could start to recover and the water table would slowly rise
521 to earlier levels. The study compared the obtained results with the previous studies that investigated
522 within particular location inside the region the values are close to each other.

523 The study identifies a lack of groundwater management in the region, primarily due to
524 overexploitation of subsurface water resources. Employing GMS software with MODFLOW 2000
525 solver, the three-dimensional groundwater flow model provides valuable insights into the aquifer
526 system of the unconfined aquifer in Erbil basin, Kurdistan region, Iraq. The study concludes that
527 average groundwater recharge values range between (0.000375-0.00037597459) m/day. Model
528 calibration utilized trial and error, automated methods, and PEST pilot points, demonstrating a
529 mean residual error (ME) of -0.03, mean absolute error (MAE) of 0.24, and root mean square error
530 (RMSE) of 0.36. The coefficient of determination (R^2) of 0.999 underscores the model's excellent
531 correspondence with field observations. Additionally, the average groundwater flow velocity is
532 estimated at approximately (0.008459) m/day, aligning with values reported in comparable studies
533 conducted in the region. Overall, the study contributes to a comprehensive understanding of
534 groundwater dynamics in the Erbil basin, emphasizing the need for sustainable water management
535 practices.

536 **5. Conclusion**

537 The hydrological study was carried out on Erbil basin region, which covered an area of about 3200
538 Km². From the results obtained in the water budget assessment for Erbil basin, the long-term
539 observations of the following hydrological parameters had been estimated for the periods of 25
540 years, then each element of the precipitation, the evaporation, and surface runoff had been
541 computed. Meanwhile, the amount of the water demand for the present and future years also was
542 estimated. The study concluded that there was a lack in water demand in the study area, which was
543 mainly due to increasing population density and their requirement for water consumptions, the
544 research also assessed that the poor management and the rate of input data was much less than the
545 water that was pumped out from the aquifers in the area, which led to producing less amount of
546 water availability than the people's requirement for water. The continuous overexploitation of the
547 amount of groundwater without management would cause water scarcity and drought problems in
548 the near future. At the end of the study, it was highly recommended that the water resources in Erbil

549 basin needed to be kept sustainable and developed for future generations and to follow the steps of
550 sustainability. The hydrological study and assessment of the water budget for the Erbil Basin would
551 provide valuable insights into the availability, distribution, and sustainability of water resources
552 within the basin, guiding decision-making for water resource management and planning. These
553 were all the main goals of the present investigation, which had been to study the hydrological data
554 from the Erbil catchment area in the northern part of Iraq and apply the budget equation to evaluate
555 the basin conditions. This had been conducted possible by a systematic hydrological study that had
556 been carried out in the research area. The study successfully demonstrated the capability of GMS
557 software in accurately simulating groundwater levels within the Erbil basin. However, it
558 acknowledges several limitations that impact the depth of understanding of the aquifer system. The
559 primary challenge lies in the lack of comprehensive data, particularly the absence of dedicated
560 observation wells, as all monitored wells serve production purposes. This limitation hampers the
561 ability to precisely verify the actual groundwater table within the model region and highlights the
562 scarcity of essential system properties.

563 **Acknowledgement**

564 This paper is apart of the phd study that is conducted on Erbil basin

565 **References**

- 566 Ahmed R. S. (2012), Geographical Analysis of Environmental Problems in Erbil basin, *Degree of*
567 *Master of Science in geography*, Erbil, Iraq (Unpublished Thesis).
- 568 Al-Areedhi HH, Khayyun TS (2019). Modelling of Groundwater Flow for the Iraqi Aquifers. PhD.
569 University of Technology.
- 570 AL-Kubaisi, Q. Y. (2008), Groundwater Chemistry of The Plio-Pleistocene Aquifer of Erbil
571 Hydrogeologic Basin, N. Iraq, *Iraqi Journal of Science*, **49(2)**, 140-148.

- 572 Al-Kubaisi, Q. Y., Hussain, T. A., Ismail, M. M., and Abd-Ulkareem, F. A. (2019), Estimation of
573 water balance for the central basin of Erbil plain (north of Iraq), *Engineering and Technology*
574 *Journal*, **37(1)**, 22-28.
- 575 Al-Sudani H.I.Z. (2018), Calculating of Groundwater Recharge using Meteorological Water
576 Balance and Water level Fluctuation in Khan Al-Baghdadi Area, *Iraq Journal Science*, **59(1B)**
577 ,349-359.
- 578 Al-Sudani H.I.Z. (2018), Study of Morphometric properties and Water Balance using Thornthwaite
579 method in Khanaqin Basin, East of Iraq, *Journal of University of Babylon, Engineering*
580 *Sciences*, **26(3)**, 165-175.
- 581 Al-Sudani, H. I. Z. (2019), Estimation of water balance in Iraq using meteorological data, *Int J*
582 *Recent Eng Sci*, **6(5)**, 8-13.
- 583 Anderson MP, William WW, Randall JH (2015). Applied Groundwater Modeling: Simulation of
584 flow and Advective Transport. Academic press, ISBN 978-0-12-058103-0
585 <http://dx.doi.org/10.1016/B978-0-12-058103-0.00001-0>.
- 586 Dizayee, R. H., (2014), Groundwater Degradation and Sustainability of the Erbil Basin, Erbil,
587 Kurdistan Region, Iraq, Master, *Texas Christian University*
- 588 Freeze RA, Cherry JA (1979). Groundwater, Prentice-Hall, Inc., Englewood Cliffs, NJ, :604
- 589 Hamad R. (2022), Erbil Basin Groundwater Recharge Potential Zone Determination Using Fuzzy-
590 Analytical Hierarchy Process (AHP) in North Iraq, *Tikrit Journal for Agricultural Sciences*,
591 ISSN:1813-1646 (Print); 2664-0597 (Online)
- 592 Hassan H. A. (1981), Hydrogeological conditions of the central art of the Erbil Basin,” Ph.D.
593 Thesis, *Baghdad University*, Iraq, p: 180.
- 594 Hassan I. O. (1998), Urban Hydrology of Erbil City Region, Ph.D. Thesis, *Baghdad University*,
595 Iraq, p: 121.

- 596 Hassan, R. M. (2022), Water budget analysis and long-term groundwater depletion in Kapran sub
597 basin, Erbil, Iraq. *Degree of Master Hydrogeology Department, University of Miskolc, Faculty*
598 *of Earth Science and Engineering* (Unpublished thesis)
- 599 Henderson A., (2012), The Future of the World's Climate, Henderson-Sellers. A. and McGuffie, K.
600 (eds), Second Edition. *Elsevier, Boston*, pp 531- 62.
- 601 Jalal H. B. (2022), Hydrogeological and Hydrochemical Study of Eastern and Western Parts of
602 Erbil City, Kurdistan Region-Iraq, *Degree of Master of Science in Earth Sciences and*
603 *Petroleum* (Unpublished thesis)
- 604 Jwan, S. M., Salah, F. S. A., and Shuokr, Q. A., (2021), Assessment of sustainability and
605 management for groundwater source in Erbil city, *Recycling and Sustainable*
606 *Development*, **14(1)**, 41-50.
- 607 McDonald MG, Arlen WH. (1988). A modular three-dimensional finite-difference ground-water
608 flow model. US Geological Survey.
- 609 Nanekely, M., Al-Faraj, F. and Scholz, M., (2019), Estimating Groundwater Balance in the
610 Presence of Climate Change Impact: A Case Study of Semi-Arid Area, *Journal of Bioscience*
611 *and Applied Research*, **5(4)**, pp.437-455.
- 612 Rafaat O. A. (2023), Hydrological Study of Catchment Area of Proposed Bastora Dam, Erbil
613 Governorate-Iraqi, Kurdistan Region, Degree of Master of Science *in Earth Sciences and*
614 *Petroleum*. (Unpublished thesis)
- 615 Smail R.Q., 2022, Evaluation of Groundwater Vulnerability of Erbil Central Sub-Basin by
616 DRASTIC Method (Iraq), *Degree of Master in Department of Geological Engineering Van*
617 *Yuzuncu Yil University Institute of Natural and Applied Science*. (Unpublished thesis)
- 618 Stevanovic Z. and Markovic. M (2004). Hydrogeology of northern Iraq, Vol. 2: General
619 hydrogeology and aquifer system, *spec. edn. (spec. Emerg. Prog. Serv.)*, Food and Agriculture
620 *Organization of the united nations (FAO), Rome*, p.69.